

# Three-Dimensional Architecture of the Mouse Tongue Muscles Using Micro-CT with a Focus on the Transverse, Vertical, and Genioglossus Muscles

Hidekazu Aoyagi<sup>1\*</sup>, Shin-ichi Iwasaki<sup>2</sup>, Tomoichirou Asami<sup>3</sup>

<sup>1</sup>Advanced Research Center, School of Life Dentistry at Niigata, The Nippon Dental University, Niigata, Japan

<sup>2</sup>Department of Physiology, School of Life Dentistry at Niigata, The Nippon Dental University, Niigata, Japan

<sup>3</sup>School of Medical Technology, Gunma Paz College, Gunma, Japan

Email: \*[aoy@ngt.ndu.ac.jp](mailto:aoy@ngt.ndu.ac.jp)

Received 8 July 2015; accepted 28 July 2015; published 31 July 2015

Copyright © 2015 by authors and Scientific Research Publishing Inc.

This work is licensed under the Creative Commons Attribution International License (CC BY).

<http://creativecommons.org/licenses/by/4.0/>



Open Access

---

## Abstract

**Background:** The suitability of micro-computed tomography (CT) for soft tissue applications has been well documented. Although the application of micro-CT to the three dimensional (3D) structure of the tongue muscle has been reported, a 3D rendering and/or a schematic view of the tongue muscle has yet to be published. **Material and Method:** First, mouse tongues were fixed and decalcified, and then the vertical muscle (Ve), the transverse muscle (Tr), and/or the genioglossus muscle of the mouse tongue (Ge) were analyzed using micro-CT and are shown in this report in rendered images and pattern diagrams. **Results:** 1) The Tr is classified into three parts: the first part extends from the middle to the apical part of the tongue; the second part is strongly connected to the superior longitudinal muscles of the tongue (Lo); the third part fans out from the middle to the root of the tongue. 2) The Ve is classified into two main groups: the first group joins the dorsal and the lateral parts of the tongue; the second group joins the dorsal part and the floor of the tongue. 3) Ge is classified into four parts: three parts comprise the Ge apical and middle parts of the tongue, with one part in the inferior longitudinal muscles of the tongue, one joining the lingual septum of the tongue (LS), and the other joining the sub-surface of the dorsal part of the Lo. The remaining Ge exits in a fan-like manner through the root of the tongue and then joins the Tr.

## Keywords

Tongue Muscles, Micro-CT, Three-Dimensional Architecture, Transverse Muscle, Vertical Muscle, Genioglossus Muscle

---

\*Corresponding author.

## 1. Introduction

The anatomical structure of the tongue is well known. In fact, anatomical and histological studies of the tongue were conducted as early as the second century [1], and many reports about the tongue survive to the present [2] [3]. Despite a long period of limited interest in the tongue, recent morphological studies of human [4] and animal tongues [5]-[8] have focused on their function. Studies of tongue function in animals such as the chameleon and the toad [9]-[12] are examples. In particular, many physiological and anatomical studies [13]-[15] have also focused on the function of the tongue in actions such as speaking, swallowing, and eating. A previous study on the structural details of the tongue muscle focused on tongue muscle innervation [16]. It was interesting that the above-mentioned paper did not include detailed information about the structure of the tongue despite the need for a physiological study of this aspect. The main reason could be that no new observational methods have been developed that are suitable for studying the complex structure of the tongue. No previous study has considered that 3D observations have greater amounts of morphological information than two dimensional (2D) images [17]-[19]. Recent 3D morphological studies of the tongue muscles were accomplished primarily using macro-anatomical [4] [20]-[22], histological [1] [6], CT [23], MRI [13] [24] [25], and ultrasound methods [26]. However, most of these methods do not display histological resolution. However, Aoyagi *et al.* showed the appropriateness of observations made using micro-CT [19], although he did not provide 3D images of individual tongue muscles. By contrast, reptilian tongues, such as that of the chameleon, have been successfully illustrated [5]. Rendered images similar to those shown in [27], in addition to illustrations, provide an improved depiction of the tongue structure. Recently, Aoyagi [28] showed images of mouse tongue muscles, such as the superior longitudinal muscle of the tongue (sLo), the hyoglossus muscle of the tongue (Hyo), the inferior longitudinal muscle of the tongue (iLo), and the styloglossus muscle of the tongue (Sty), which were processed by rendering methods, but a complete image of the tongue was not included. The aim of the present study was to fill this gap in the images of the tongue muscles by providing information about the transverse muscle of the tongue (Tr), the vertical muscle of the tongue (Ve), and the genioglossus muscle of the tongue (Ge).

## 2. Materials and Methods

### Animals and Experimental Procedures

The animal experiments were performed in accordance with the guidelines for animal experiments at Nippon Dental University's School of Life Dentistry at Niigata. Four 3-month-old male mice (Slc:ddY, Hamamatsu, Japan, average weight 45 g) were used in this study. They were killed using an intraperitoneal overdose of sodium pentobarbital (200 mg/kg body weight). The head portions with tongues were fixed in 4% formaldehyde for one week at room temperature. The tongues were then separated from the heads and decalcified in decalcifying solution A (Plank-Rychlo; Wako, Osaka, Japan). After alcohol dehydration, T-butyl alcohol substitution was performed. The tongues were then freeze-dried in a freeze dryer (ES-2030; Hitachi, Hitachi, Japan).

The image-processing specimens were scanned using a micro-CT system (SMX-100CTSV, Shimadzu, Kyoto, Japan) as follows: X-ray source 22 kv, 57 mA, pixel size 512, 512, source to object distance (SOD) 37.6 mm, source to image-receptor distance (SID) 179.7 mm (**Figure 1(A)**, 5); X-ray source 22 kv, 83 mA, pixel size 512, 512, SOD 13.3 mm, SID 216.3 mm (**Figure 1(B)**, **Figure 1(C)**, 2, 3); and X-ray source 22 kv, 56 mA, pixel size 512, 512, SOD 17.5 mm, SID 179.8 mm (**Figure 1(D)**, 4). The micro-CT images were then reconstructed using 3D structural analysis software (MPR, Shimadzu, Kyoto, Japan and TRI/3D BON and FCS4D/VOLvie, Ratoc System Engineering, Tokyo, Japan).

In the process of image rendering, most images were made manually, focusing on consecutive muscle fibers (fascicles) in the 3D structure and then grouping each muscle in the tongue. Rendering the images of tongue muscles, such as sLo, iLo, Hyo, and Sty, which are processed automatically, is beyond the focus of this study.

## 3. Results

### 3.1. Extraction of the Image Object

The tongue muscles and their surrounding tissues were recorded using micro-CT and the Aoyagi method [19]. Two types of observations were performed: high magnification of the muscle fascicle images (**Figures 1-3**) and low magnification of the pattern diagram (**Figure 4**) of the entire tongue image. This study focused on the

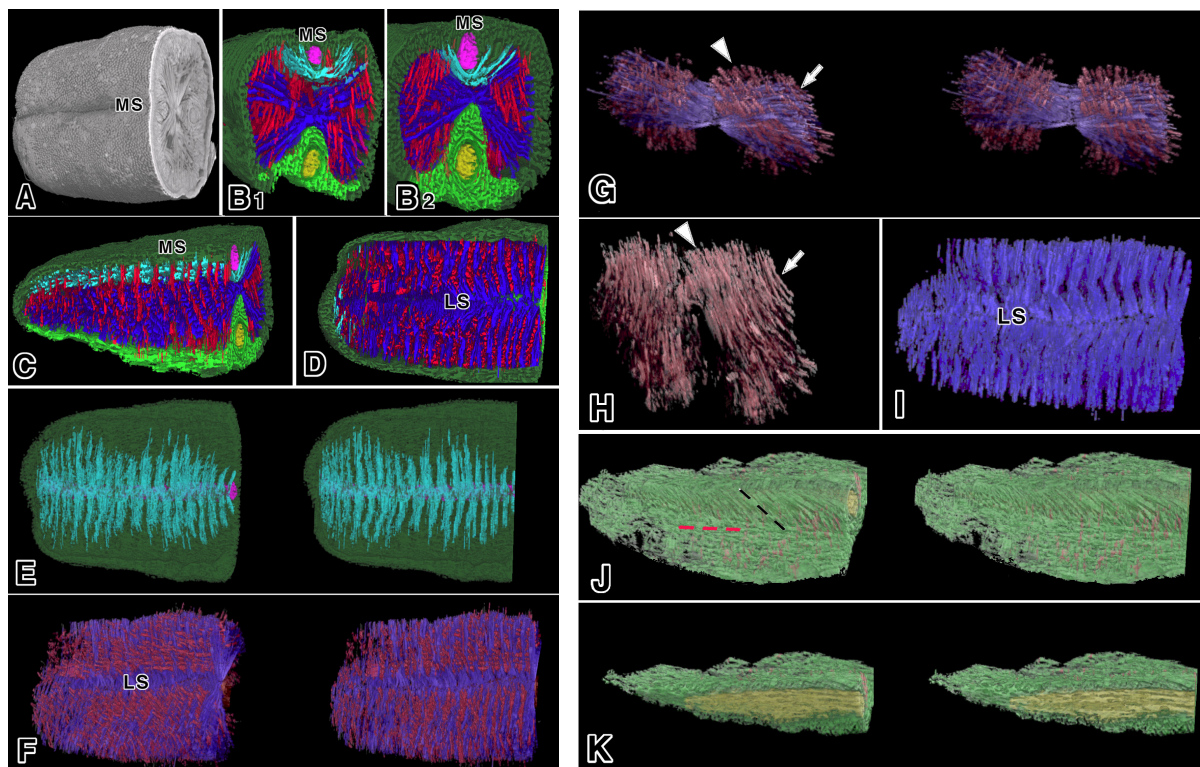


**Figure 1.** Apical part of the tongue using micro-CT. Deep green, sLoG; green, iLoG; red, Ve; blue, Tr; Ge, yellow; pink, mMS. Stereo pairs of images; Bar: 10  $\mu$ m. (A) tongue image of micro-CT before image processing; (B<sub>1</sub>) apical side cut face and (B<sub>2</sub>) middle side cut face in (A) after image processing; (C) surgical cut image in (B); (D) horizontal cut image in (B); (E) bottom view of mMS and cTr; (F) bottom view of Tr and Ve. (G) frontal view of parts of Ve and Tr; (H) frontal view of part of Ve; (I) bottom view of Tr; (J) upper view of iLoG; (K) Surgical cut image in (J).

muscle fascicles of the genioglossus muscle of the tongue (Ge, yellow), the vertical muscle of the tongue (Ve, red), and/or the transverse muscle of the tongue (Tr, green). Tr, Ve, and Ge were extracted from the micro-CT data and then marked with the appropriate color on the raw micro-CT images (Figures 1-3). They were then shown as pattern diagrams of the tongue muscle with other muscles (Figure 4). Other tongue muscles (other than Tr, Ve, and Ge) were displayed according to Aoyagi [28]; the superior longitudinal muscle of the tongue (sLo) and the hyoglossus muscle of the tongue (Hyo) were considered to make a muscle set in the sLo group (sLoG, deep green). Similarly, the inferior longitudinal muscle of the tongue (iLo) and the styloglossus muscle of the tongue (Sty) were considered to make a muscle set in the iLo group (iLoG, deep green). Muscle bundles exist under the median sulcus of the tongue (MS), shown as mMS (pink). Above these muscles, the hyoid bone (HB, white) was also extracted from the micro-CT data and marked with the appropriate color on the raw micro-CT images (Figures 1-3). In conjunction with the Tr (cTr, aqua), an unknown structure (mentioned later) was also painted in the micro-CT images. Another unknown structure (also mentioned later) appeared in conjunction with the circumvallate. It was named cCP (pink) and painted in micro-CT images. In this research, the epithelial images, vessels and the nerves were cropped by image processing. In several cases, stereo pairs of the reconstructed images were used to clarify the real 3D images.

### 3.2. Observations of the Apical Part of the Tongue

Using micro-CT, the apical part of the tongue (Figure 4(A), as positioned) was shown as a macro gross image (Figure 1(A)). The cut face of the tongue structure indicated that it was constructed from the muscle fascicles. Tr (green), Ve (red), Ge (yellow), sLoG (dark green), iLoG (brown), mMS (pink), and cTr (aqua) were identified and painted. Two frontal cuts of the tongue were made: the left cut was near the apical side; and the right cut was on the middle side of the tongue (Figure 1(B<sub>1</sub>), Figure 1(B<sub>2</sub>)). A surgical cut and a horizontal cut were

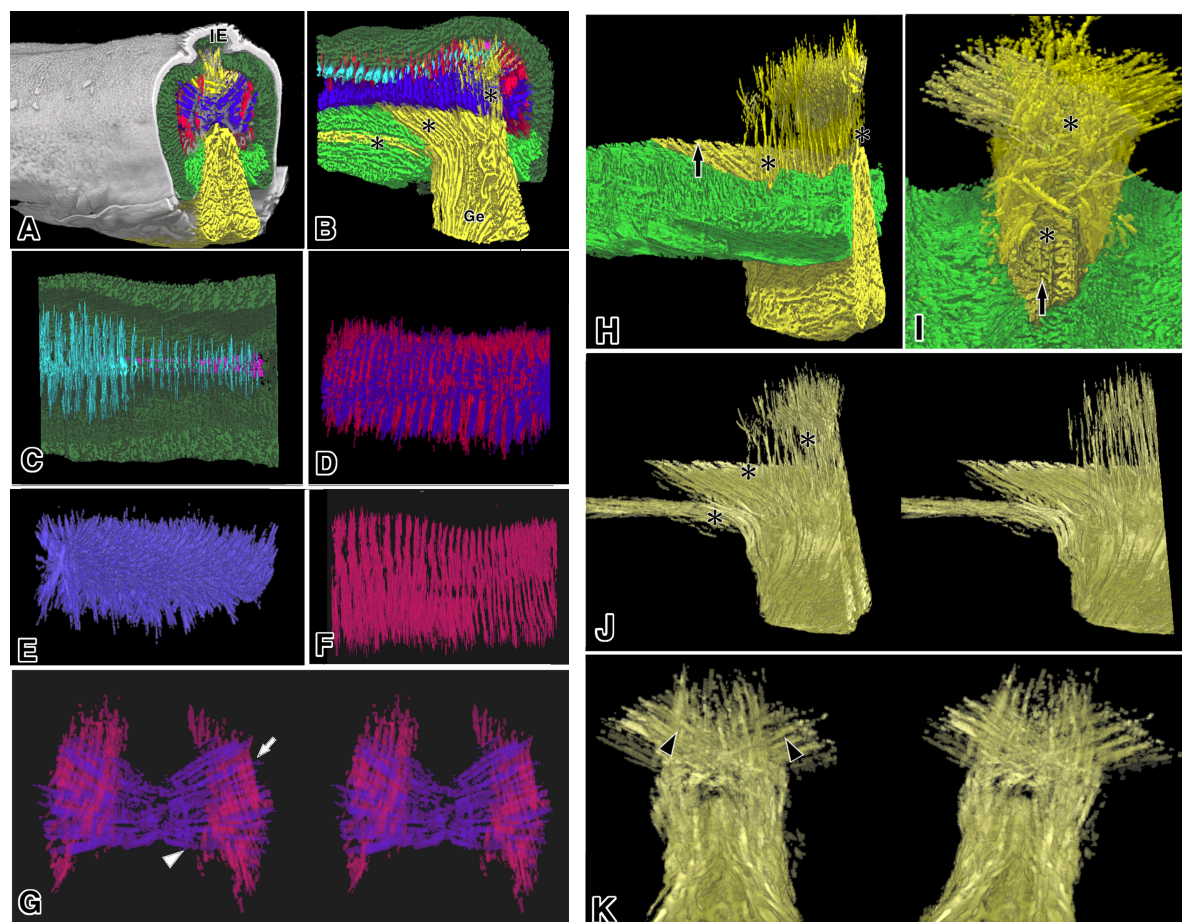


**Figure 2.** Middle part of the tongue using micro-CT after image processing. Deep green, sLoG; green, iLoG; red, Ve; blue, Tr; yellow, Ge; pink, mMS. Stereo pairs of images. Bar: 10  $\mu$ m. (A) tongue image of micro-CT after image processing with epithelium; (B) surgical cut image of (A); (C) bottom view of mMS and cTr; (D) lateral view of Tr and Ve; (E) same view of Ve in (D); (F) same view of Tr in (D); (G) front diagonal view of units Tr and Ve. (H) lateral view of part of iLoG and part of Ge; (I) front view of (H); (J) lateral view of Ge; (K) back view of (H); (L) same image as in (K) showing other muscles.

made near the lingual septum (LS) of the tongue (**Figure 1(C)**, **Figure 1(D)**). The local relation of Tr and Ve in the tongue was clearly recognizable, as shown in **Figures 1(B)-(D)**. The structure of cTr (aqua), which was previously unnamed, was named in this study (Abbreviations). It bordered Tr (**Figure 1(B<sub>1</sub>)**) or was near Tr (**Figure 1(B<sub>2</sub>)**). Consequently, cTr and Tr at the apex side joined at the middle part of the tongue. These relationships are shown in the pattern diagrams in **Figure 4(B)**. Because the structure and function of cTr were similar to Tr, it had been considered the same as Tr. In order to clarify the relation between cTr and Tr, the upper part of the tongue that contained cTr, mMT, and/or sLoG was separated by the image analyzer and viewed from the bottom side. The view showed that cTr had a joint function between both sides of sLoG. mMT (pink) was viewed weakly under the cTr (**Figure 1(E)**). When the relations between Tr and Ve were viewed separately from the bottom side, the stratified formation of Tr and Ve was clearly recognizable (**Figure 1(F)**). Part of the stratified units of Ve and Tr was viewed from the upper-frontal position (**Figure 1(G)**). Ve (**Figure 1(H)**) and Tr (**Figure 1(I)**) were viewed alone. The relation between Tr and Ve was well shown in the image, and two types of Ve muscle fascicles were recognized. Two patterns of Ve fascicles were grouped. One was near the corner of the tongue (**Figure 1(G)**, **Figure 1(H)** arrow), running from the dorsal part laterally; the other one was near the center of the tongue (**Figure 1(G)**, **Figure 1(H)** arrow head), running from the dorsal part to the base. The shape of the Tr unit was similar to a fan and spread from the LS. However, they were not on the same plane, and they continuously slipped from each other from the apical to the middle parts of the tongue (**Figure 1(I)**). These relations are shown in the pattern diagrams provided in **Figure 4(A)**. The floor part of the tongue mainly contained

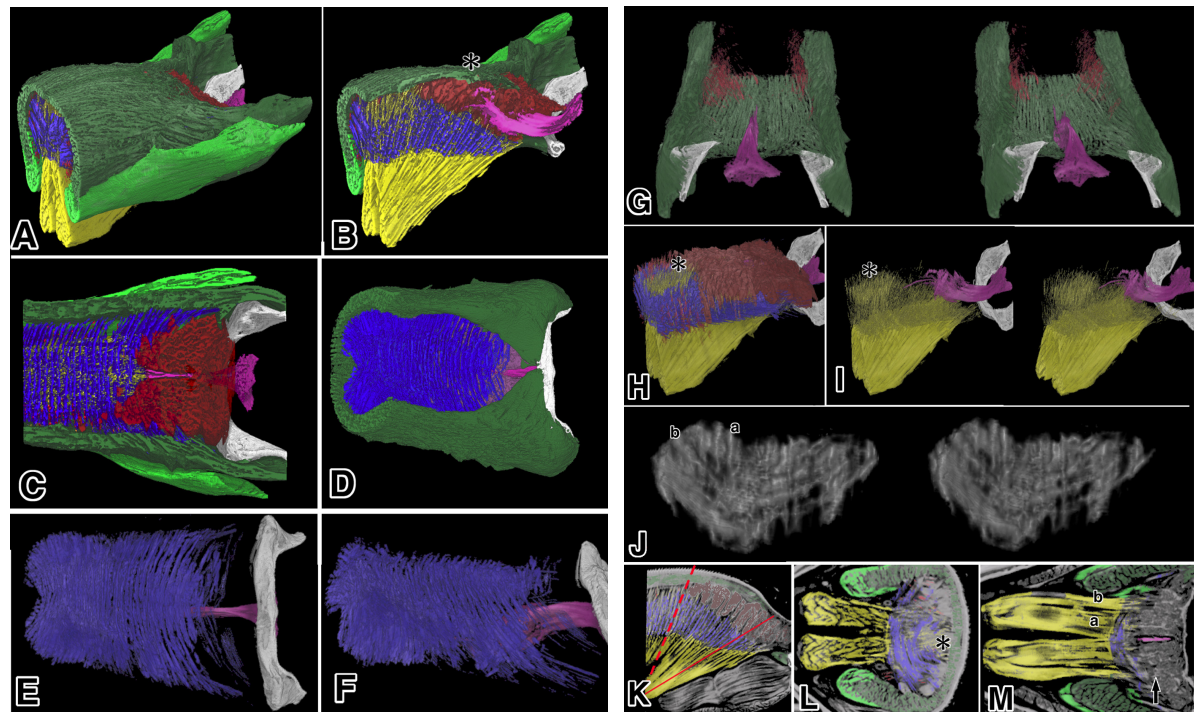


**Figure 3.** Root part of the tongue using micro-CT. Deep green, sLoG; green, iLoG; red, Ve; blue, Tr; yellow, Ge; pink, mMS. Stereo pairs of images. Bar: 10  $\mu$ m. (A) tongue picture of micro-CT after image processing; (B) surgical cut image of (A); (C) horizontal view of (A); (D) bottom view of (A) after Ge removal; (E) top view of Tr; (F) lateral view of (E); (G) back bottom image focused on Ve; (H) lateral view of (A) after removal of iLoG and sLoG; (I) same view of Ge in (H) (J) front view of unit Tr and Ge in a raw image, a:Ge, b:Tr; (K) semi-surgical cut image of tongue; (L) cut face of red back line in (K); (L) cut face of red line in (K). (G) back bottom image focused on Ve; (H) lateral view of (A) after removal of iLoG and sLoG; (I) same view of Ge in (H); (J) front view of unit Tr and Ge in a raw image, a:Ge, b:Tr; (K) semi-surgical cut image of tongue; (L) cut face of red back line in (K); (L) cut face of red line in (K).

Ge and iLoG (**Figure 1(J)**, **Figure 1(K)**). The part of the Ge inside the iLoG is shown in **Figure 1(K)**. The iLoG was composed of two structures: one structure consisted of the muscle fascicles that run parallel to the long axis of the tongue (**Figure 1(J)**, broken red line); the other one runs around Ge and is oblique to the long axis of the tongue, connecting to the LS (**Figure 1(J)**, broken black line).

### 3.3. Observation of the Middle Part of the Tongue

The middle part of the tongue (**Figure 4(A)**, as positioned) was analyzed in the same way as the apical part. It was also revealed by a frontal cut, which added epithelium and the intermolar eminence (IE) [29] (**Figure 2(A)**), and by a surgical cut (**Figure 2(B)**). It was found that Ge (yellow) had three types of muscle fascicles (**Figure 2(B)**, \* mark): one fascicle was in the iLoG (green); one fascicle was connected to Tr (blue) or LS (blue); and the remaining fascicle was connected to the iLoG, or it ran under the IE. The broad-based area of Ge (**Figure 2(B)**, Ge mark), which was connected to three types of Ge and is seen as a form outside the tongue body, had only a Ge component. Therefore, the rendering of the Ge muscle fascicle in this area was done automatically, not manually. The image showed that the amount of Ge muscle outside the tongue body was greater than the other three types of Ge. Hence, in this study, the quantities of information about the muscle fascicles were uncertain. It was also found that cTr (aqua) diminished as it moved to the root side of the tongue. This observation is shown in **Figure 2(C)** and in **Figure 1(D)**. The size of the cTr was reduced, and it mixed with the Tr and/or the LS as it reached the root side. The separate views in the images of Tr and Ve show the lateral view (**Figure 2(D)**), the frontal view of Tr alone (**Figure 2(E)**), the same frontal view of Ve alone (**Figure 2(F)**), and the frontal view of Tr and Ve in one unit (**Figure 2(G)**). These relationships were almost the same as in the apical part of the tongue, except Ge. Two types of muscle fascicles in the Ve (**Figure 2(G)**, arrow and arrowhead) were also found to be partly the same as the apical part of the tongue, but the Ve on the center side diminished

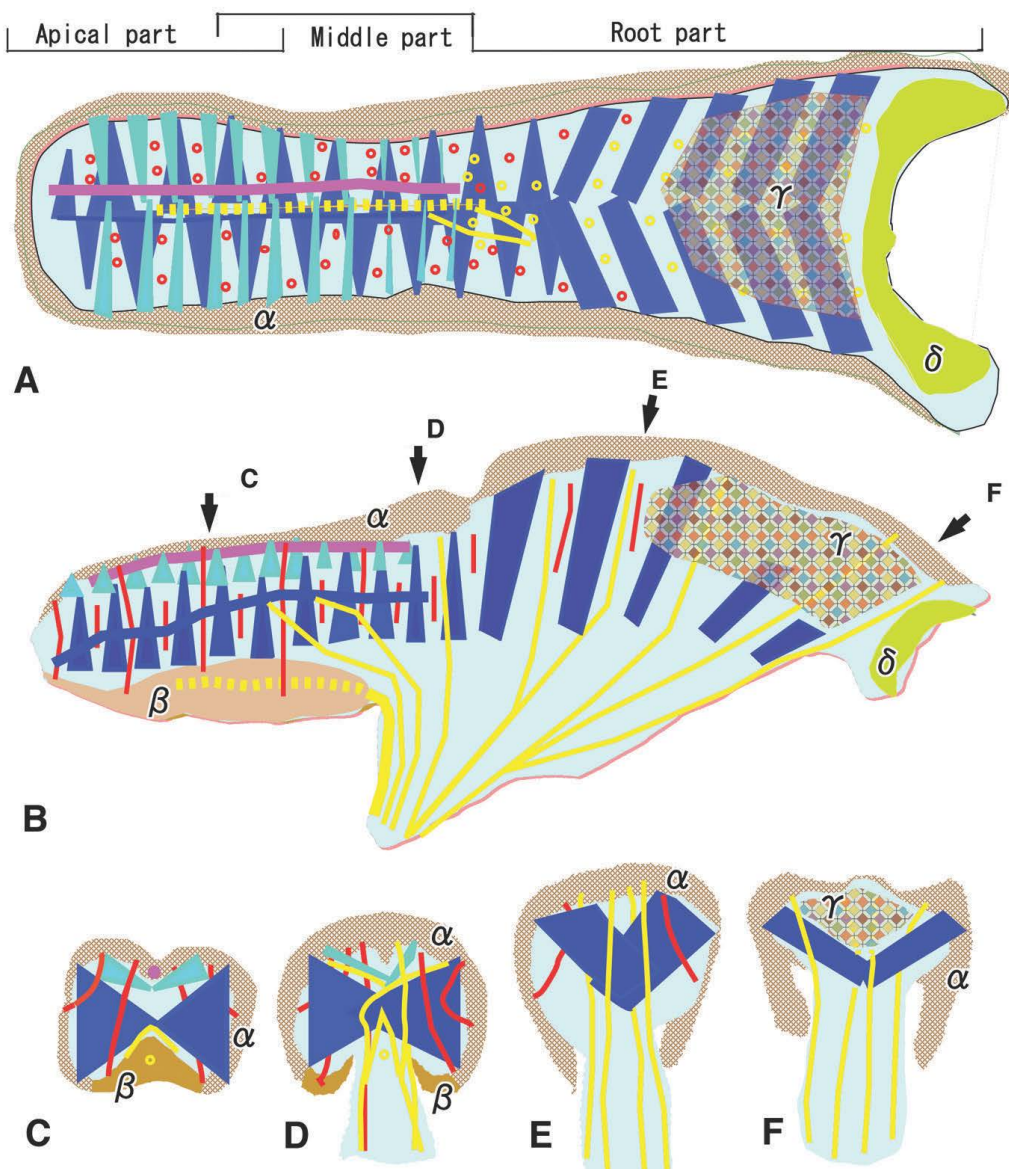


**Figure 4.** Diagram of the muscles in the tongue focused on Tr, Ve, and Ge. Blue, Tr; Ve, red; yellow, Ge; aqua, cTr; pink, mMS;  $\alpha$  sLoG;  $\beta$ , iLoG;  $\gamma$ , Gl;  $\delta$ , HB; (A) horizontal image of symbolized muscles, (B) lateral image of symbolized muscles (C)-(F); cut face images of symbolized muscles shown by the arrows in (C)-(F).

as it moved to the root side. Ge (yellow) and iLoG (green) were separated from the other tongue muscles, but the latter was an appendix. It is shown in a lateral view (**Figure 2(H)**) and a frontal view (**Figure 2(I)**). Part of iLoG connected with the LS as shown by the broken black line in **Figure 1(J)**. In the same manner as iLoG, part of the Ge ran into the LS area and changed roles from iLoG to Ge (**Figure 2(H)**, **Figure 2(I)** arrow). The frontal view of Ge alone clarified the relation of the third type of Ge (**Figure 2(J)**, \*mark). Part of the Ge ran laterally in the frontal view of Ge (**Figure 2(K)**, arrowhead), which occurred in a mixed muscle scramble (**Figure 2(L)**).

### 3.4. Observation of the Root Part of the Tongue

The root part of the tongue (**Figure 4(A)**, as positioned) was analyzed in the same manner as the apical part. The surgical cut and the horizontal cut are shown as the colored images in **Figure 3(A)-(C)**. It was found that Ge (yellow) spread in a fan-like structure and ran into the Tr (blue), stopping at sLoG (dark green) and/or the glan-

dular tissue (GI; brown). In the other tissue, the Ge was manually selected. However, some muscle fascicles in Ge were difficult to identify as Ge because it was uncertain that the Ge fascicle continued from the base area. In this case, Ge that could not be identified was ignored. Consequently, the actual amounts of Ge in the other tissues were low, but the distribution of Ge was correct. **Figure 3(B)**, **Figure 3(H)**, and **Figure 3(I)** (\* mark) shows an unnamed structure that had a small plate in the center, which ran from under the circumvallate papilla (CP) to over the HB (white). This structure was temporarily named cCP (in conjunction with the circumvallate papilla shown in pink). The cCP was a good marker of the position of tongue tissue and could have a functional relation with the tongue muscles (**Figure 3**). The distribution and structure of Tr (blue) through the tongue are shown clearly in **Figure 3(A)-(C)**. Even clearer information about Tr is shown in the bottom view, which was obtained by removing the Ge (**Figure 3(D)**). The bottom and lateral views composed of Tr, cCP, and/or HB (white) are shown in **Figure 3(E)** and **Figure 3(F)**. The Tr that occupied most of the inside space of the sLoG was viewed as a wraparound and regular-pattern layered structure. The layers were steadily bent along the Ge fan-like structure. The width of the unit structure of Tr narrowed as it crossed to HB because of the presence of GI. The distribution of Ve (red) was viewed in conjunction with sLoG (deep green), cCP (pink), and HB (white) (**Figure 3(G)**). Ve ran on the angular part of the tongue, and the amount of Ve decreased, and it dispersed as it approached the root. Similar to the Ge in the other tissue, the amount of Ve was also uncertain. To clarify the structure of Ge (yellow), a lateral view of Tr, GI, HB, and cCP (**Figure 3(H)**) and a lateral view of HB and cCP (**Figure 3(I)**) were made. The unit structure of Tr with Ge was determined without rendering the image in processing (**Figure 3(J)**), and frontal-like cut images of the Ge in other tissue (**Figures 3(K)-(M)**) were made. The continuity of the Ge fascicle and its direction are shown in **Figure 3(I)**. However, a comparison among **Figure 3(A)-(C)**, **Figure 3(H)**, **Figure 3(I)**, and **Figures 3(K)-(M)** was needed to obtain the Ge images. The relationship between Tr and Ge was complex, because they were partially interwoven (**Figure 3(J)**), a: Ge, b: Tr). The relationship between Ge and Tr was easy to understand in the cut face. In the GI area, it appeared that part of Ge ran into the GI. However, the line that resembled Ge was irregular (**Figure 3(M)**, \*arrow). Thus, in this study, this irregular structure was ignored and considered part of the GI structure.

### 3.5. Summarized Model of Tongue Muscles

The three-dimensional structural properties of Tr, Ve, and Ge in the tongue muscle were summarized as pattern diagrams in the horizontal, lateral, and frontal views (**Figure 4**):

About Tr (blue): There were three types of Tr. The first type was expressed as several triangle planes. It was anchored by LS, and it was viewed from the apical to the center parts of the tongue (**Figure 4(A)**). The second type was cTr (named in this study), which was similar to Tr. It was expressed as many thin triangle planes (aqua), and it was attached to sLoG (**Figure 4(A)**, **Figure 4(C)**). It existed apart from Tr in the apical part, but was near Tr in the center part of the tongue (**Figures 4(B)-(D)**). The third type was seen as many square planes that changed arrangement and width (**Figure 4(A)**, **Figure 4(E)**, **Figure 4(F)**).

About Ve (red): property. There were two types of Ve. The first type was symbolized in the many lines that joined the dorsal part and the lateral part of the tongue. It extended apart from the apical through the center to the middle of the root part of the tongue (**Figures 4(B)-(E)**). The second type of Ve joined the dorsal part and floor of the tongue. It extended apart from the apical part to the center part of the tongue.

About Ge (yellow): There were four types of Ge, which were shown in the images as many lines. The first type ran mainly in the iLoG (**Figure 4(B)**). The second type connected with LS and/or Tr (**Figure 4(B)**). The third type connected with sLoG and ran under the IE. Part of its Ge crossed over the second Ge near the center part of the tongue (**Figure 4(D)**). The fourth type ran into the Tr, and it terminated at sLoG and the boundary of GI (**Figure 4(B)**, **Figure 4(F)**).

## 4. Discussion

### 4.1. Methods

Few studies have focused on the macromorphological study of the tongue muscle. The reason is that most researchers assume that this area has been investigated [19] [28]. However, precise structural information about the tongue muscles exists only in textbooks, but not in recent reports. The main reason for the lack of information about the structure of the tongue is the difficulty of observing this complex muscle structure. For example,

the separation of the unit muscle from the tongue is impossible. Consequently, most knowledge has been gained by observing images of the cut faces. No information about the reconstruction of the tongue muscle by serial section is available. Takemoto (2008) [30] cut a monkey's tongue into several pieces and then constructed a 3D model of the muscle after macromorphological observation. However, compared to the present results, it is difficult to extract muscle units for 3D display using Takemoto's method. Thus, although the use of 2D images is limited, several methods for the observation of the tongue muscle, such as MRI [13] [24] [25], are known [19]. When the aim is to reconstruct the muscle unit of the tongue, structural information is required about the resolution of the muscle fascicle. At present, in the case of mouse, micro-CT methods are used to achieve high resolution [17]-[19] [28]. MRI allows the direction of the muscle fascicle to be obtained easily and the muscles to be rendered [31], but the histological resolution is not sufficient, because results of previous studies using MRI methods that are similar to the present results were not found.

#### 4.2. Results of Observations of Tr, Ve, and Ge

Previous studies related to the present results could not be found except for our recent research [28], which showed iLoG and sLoG as 3D-rendering images. Hence, the main remaining muscles of the tongue, such as Tr, Ve, and Ge were summarized.

Tr is divided into three groups. Unit Tr is spread from LS, and many Tr units are arranged in a zigzag formation from the apex to the middle part of the tongue. These images are considered the main structure of the inside of the tongue. The newly named cTr is considered a part of the Tr group because its unit structure and arrangements are similar to Tr but have no relation to LS. The other Tr, which extends apart from the center to the root part of the tongue is divided from the main Tr, because its arrangement does not resemble the main Tr, and it has no relation to LS. Moreover, it is suspected that the existence of three types of Tr structure has a strong relation to muscle formation and the branchial arch in morphological development. Regarding the type of Tr, there are many illustrations of frontal cut images [2] [3], but few are in the direction of the long axis [32]. The results of these previous studies do not align with our results.

Ve is divided into two groups that are shown as symbolized images in the pattern diagrams. They exist mainly between unit Trs, and they are not arrayed on the surface structure. This division was made by emphasizing two functions: the first function joins the dorsal and floor parts; and the second function joins the lateral and dorsal parts. In connection with the types of Ve, Sokoloff and Smith (2013) [33] showed three types of Ve in rat through diagrammatic representations. The results of this study align with our results.

Ge is divided into four groups. To examine the types of Ge, Mu and Sander (2000) [16] used dog for innervation patterns in Ge. They used all GG muscles with Sihler's stain for the muscle observations. Their results showed that Ge was divided into three types as follows. The former extended into and controlled the apex side of the tongue, and the latter ran vertically and transversely into the horizontal and oblique compartments, respectively. The results of our observation of the Ge in the apex side of the tongue were in agreement [16], but our other results did not. This difference was caused by the species differences and/or observation methods. Using the tongue of a 15-week-old human fetus, Langdon *et al.* (1978) [34] found a cross arrangement of Ge in the center part of the tongue, which agrees with our results. In the Tr of the root of the tongue, it is difficult to select all of the Ge because the Tr and Ge are intertwined. However, the present results showing their basic arrangement are valid. It is suspected these four Ges have independent functions in the movement of the tongue.

#### 4.3. Analysis of the Images of the Tongue Muscle

The general analysis of the entire range of images is beyond the scope of this report. Hence, problems related to the tongue muscle are discussed here. When the muscle unit, such as Ge in Tr, was divided from micro-CT data, it was impossible to use automatic selection. Miyawaki [35] focused on the direction of the muscle fascicle but was unable to obtain 3D images because his data were not computerized. For the division of the muscle, the fascicles were also used in the image rendering, but the process was difficult because no software is available. Most analyses of the images were done manually and focused on the muscle fascicles that run in a continuous line on the tongue. Our hypothesis that one muscle is composed of muscle fascicles that run continuously through the muscle was supported by our previous studies [19] [28]. In the case of Ge in Tr, as mentioned above, confirmation of continuity is difficult. Our future research will attempt to solve this problem by providing histological conformation. Only a mouse tongue structure was investigated here, which comprises a limitation of this study;

therefore, we plan to look at the tongue of a different animal in a future study.

## 5. Conclusion

In this study, the vertical muscle (Ve), the transverse muscle (Tr), and/or the genioglossus muscle (Ge) of the mouse tongue were analyzed by micro-CT and were presented as rendered images and pattern diagrams as follows. The Tr was classified into three parts; the Ve was classified into two main groups; and the Ge was classified into four parts. A 3D rendering and/or a schematic view of the tongue muscle was crucial for this.

## Acknowledgements

We are grateful to Prof. I. Sasagawa of the Advanced Research Center at the Nippon Dental University School of Life Dentistry at Niigata for his encouragement and constant support. We also wish to thank Prof. A. Ezura of General Dentistry at the Nippon Dental University School of Life Dentistry at Niigata for his help and suggestions. This research was supported by Research Promotion Grants [No. NDUF-14-13] from the Nippon Dental University.

## References

- [1] Barnwell, E.M. (1976) Human Lingual Musculature: An Historical Review. *International Journal of Oral Myology*, **2**, 31-41.
- [2] Clemente, C. (1985) Gray's Anatomy of the Human Body. 30th Edition, Lea & Fibiger, Philadelphia.
- [3] Schaffer, J. (1951) Collective Review, Clinical Pathology of the Tongue. *Oral Surgery, Oral Medicine, Oral Pathology*, **4**, 1287-1316. [http://dx.doi.org/10.1016/0030-4220\(51\)90088-6](http://dx.doi.org/10.1016/0030-4220(51)90088-6)
- [4] Ogata, S., Mine, K., Tamatsu, Y. and Himada, K. (2002) Morphological Study of the Human Chondroglossus Muscle in Japanese. *Annals of Anatomy*, **184**, 493-499. [http://dx.doi.org/10.1016/S0940-9602\(02\)80087-5](http://dx.doi.org/10.1016/S0940-9602(02)80087-5)
- [5] Diogo, R. (2009) The Head and Neck Muscles of the Philippine Colugo (Dermoptera: *Cynocephalus valans*), with a Comparison to Treeshrews, Primates, and Other Mammals. *Journal of Morphology*, **270**, 14-51. <http://dx.doi.org/10.1002/jmor.10666>
- [6] Smith, J.C., Goldberg, S.J. and Shall, M.S. (2006) Myosin Heavy Chain and Fiber Diameter of Extrinsic Tongue Muscles in Rhesus Monkey. *Archives of Oral Biology*, **51**, 520-525. <http://dx.doi.org/10.1016/j.archoralbio.2005.10.006>
- [7] Smith, K.K. (1988) Form and Function of the Tongue in Agamid Lizards with Comments on Its Phylogenetic Significance. *Journal of Morphology*, **196**, 157-171. <http://dx.doi.org/10.1002/jmor.1051960205>
- [8] Schwenk, K. (1994) Why Snakes Have Forked Tongues. *Science*, **263**, 1573-1577. <http://dx.doi.org/10.1126/science.263.5153.1573>
- [9] Gans, C. and Gorniak, G.C. (1982) Functional Morphology of Lingual Protrusion in Marine Toads [*Bufo Marinus*]. *American Journal of Anatomy*, **163**, 195-222. <http://dx.doi.org/10.1002/aja.1001630302>
- [10] Herrel, A., Meyers, J.J., Nishikawa, K.C. and Vree, F.D. (1986) Morphology and Histochemistry of the Hyolingual Apparatus in Chameleons. *Journal of Morphology*, **249**, 154-170. <http://dx.doi.org/10.1002/jmor.1047>
- [11] Smith, K.K. (1986) Morphology and Function of the Tongue and Hyoid Apparatus in *Varanus* (Varanidae, Lacertilia). *Journal of Morphology*, **187**, 261-287. <http://dx.doi.org/10.1002/jmor.1051870302>
- [12] Lombard, R.E. and Wake, D. (1977) Tongue Evolution in the Lungless Salamanders, Family Plethodontidae. II Function and Evolutionary Diversity. *Journal of Morphology*, **153**, 39-80. <http://dx.doi.org/10.1002/jmor.1051530104>
- [13] Sosnovik, D.E., Wang, R., Dai, G., Wang, T., Aikawa, E., Novikov, M., Rosenzweig, A., Gilbert, R.J. and Wedeen, V.J. (2009) Diffusion Spectrum MRI Odontology 123 Tractography Reveals the Presence of a Complex Network of Residual Myofibers in Infarcted Myocardium. *Circulation Cardiovascular Imaging*, **2**, 206-212. <http://dx.doi.org/10.1161/CIRCIMAGING.108.815050>
- [14] Kayalioglu, M., Shcherbaty, V., Seifi, A. and Liu, Z.J. (2007) Roles of Intrinsic and Extrinsic Tongue Muscles in Feeding: Electromyographic Study in Pigs. *Archives of Oral Biology*, **52**, 786-796. <http://dx.doi.org/10.1016/j.archoralbio.2007.01.004>
- [15] Napadow, V.J., Chen, Q. and Wedeen, V.J. and Gilbert, R.J. (1999) Intramural Mechanics of the Human Tongue in Association with Physiological Deformations. *Journal of Biomechanics*, **32**, 1-12. [http://dx.doi.org/10.1016/S0021-9290\(98\)00109-2](http://dx.doi.org/10.1016/S0021-9290(98)00109-2)
- [16] Mu, L. and Sanders, I. (1999) Neuromuscular Organization of the Canine Tongue. *Anatomical Record*, **256**, 412-424. [http://dx.doi.org/10.1002/\(SICI\)1097-0185\(19991201\)256:4<412::AID-AR8>3.0.CO;2-5](http://dx.doi.org/10.1002/(SICI)1097-0185(19991201)256:4<412::AID-AR8>3.0.CO;2-5)

- [17] Aoyagi, H., Tsuchikawa, K. and Iwasaki, S. (2010) Three-Dimensional Observation of the Mouse Embryo by Micro-Computed Tomography: Composition of the Trigeminal Ganglion. *Odontology*, **98**, 26-30. <http://dx.doi.org/10.1007/s10266-009-0112-9>
- [18] Aoyagi, H., Tsuchikawa, K. and Iwasaki, S. (2012) Three-Dimensional Observation of the Mouse Embryo by Micro-Computed Tomography: Meckel's Cartilage, Otocyst, and/or Muscle of Tongue. *Odontology*, **100**, 134-143. <http://dx.doi.org/10.1007/s10266-011-0041-2>
- [19] Aoyagi, H., Iwasaki, S. and Nakamura, K. (2015) Three-Dimensional Observation of Mouse Tongue Muscles Using Micro-Computed Tomography. *Odontology*, **103**, 1-8. <http://dx.doi.org/10.1007/s10266-013-0131-4>
- [20] McClung, J.R. and Goldberg, S.J. (2002) Organization of the Hypoglossal Motoneurons that Innervate the Horizontal and Oblique Components of the Genioglossus Muscle in the Rat. *Brain Research*, **950**, 321-324. [http://dx.doi.org/10.1016/S0006-8993\(02\)03240-7](http://dx.doi.org/10.1016/S0006-8993(02)03240-7)
- [21] McClung, J.R. and Goldberg, S.J. (2000) Functional Anatomy of the Hypoglossal Innervated Muscles of the Rat Tongue: A Model for Elongation and Protrusion of the Mammalian Tongue. *Anatomical Record*, **260**, 378-386. [http://dx.doi.org/10.1002/1097-0185\(20001201\)260:4<378::AID-AR70>3.0.CO;2-A](http://dx.doi.org/10.1002/1097-0185(20001201)260:4<378::AID-AR70>3.0.CO;2-A)
- [22] Saito, H. and Itoh, I. (2007) The Three-Dimensional Architecture of the Human Styloglossus Especially Its Posterior Muscle Bundles. *Annals of Anatomy*, **189**, 261-267. <http://dx.doi.org/10.1016/j.aanat.2006.10.002>
- [23] Stutley, J., Cooke, J. and Parsons, C. (1989) Normal CT Anatomy of the Tongue, Floor of Mouth and Oropharynx. *Clinical Radiology*, **40**, 248-253. [http://dx.doi.org/10.1016/S0009-9260\(89\)80184-9](http://dx.doi.org/10.1016/S0009-9260(89)80184-9)
- [24] Laine, F.J. and Smeker, W.R.K. (1995) Oral Cavity: Anatomy and Pathology. *Seminars in Ultrasound CT and MRI*, **16**, 527-545. [http://dx.doi.org/10.1016/S0887-2171\(06\)80024-7](http://dx.doi.org/10.1016/S0887-2171(06)80024-7)
- [25] Boom, H.P.W., van Spronsen, P.H., van Ginkel, F.C., van Schijndel, R.A., Castelijns, J.A. and Tuinzing, D.B. (2008) A Comparison of Human Jaw Muscle Cross-Sectional Area and Volume in Long- and Short-Face Subjects, Using MRI. *Archives of Oral Biology*, **53**, 273-281. <http://dx.doi.org/10.1016/j.archoralbio.2007.08.013>
- [26] Volk, J., Kadivec, M., Music, M.M. and Ovsenik, M. (2010) Three-Dimensional Ultrasound Diagnostics of Tongue Posture in Children with Unilateral Posterior Crossbite. *American Journal of Orthodontics and Dentofacial Orthopedics*, **138**, 608-612. <http://dx.doi.org/10.1016/j.ajodo.2008.12.028>
- [27] Lautenschlager, S., Bright, J.A. and Rayfield, E.J. (2014) Digital Dissection—Using Contrast-Enhanced Computed Tomography Scanning to Elucidate Hard- and Soft-Tissue Anatomy in the Common Buzzard *Buteo buteo*. *Journal of Anatomy*, **224**, 412-431. <http://dx.doi.org/10.1111/joa.12153>
- [28] Aoyagi, H., Iwasaki, S. and Asami, T. (2015) Three-Dimensional Architecture of the Tongue Muscles by Micro-CT with a Focus on the Longitudinal Muscle. *Surgical Science*, **6**, 187-197. <http://dx.doi.org/10.4236/ss.2015.65030>
- [29] Iwasaki, S., Yosizawa, H. and Kawahara, I. (1997) Study by Scanning Electron Microscopy of the Morphogenesis of Three Types Lingual Papilla in the Rat. *Anatomical Record*, **247**, 528-541. [http://dx.doi.org/10.1002/\(SICI\)1097-0185\(199704\)247:4<528::AID-AR12>3.0.CO;2-R](http://dx.doi.org/10.1002/(SICI)1097-0185(199704)247:4<528::AID-AR12>3.0.CO;2-R)
- [30] Takemoto, H. (2008) Morphological Analyses and 3D Modeling of the Tongue Musculature of the Chimpanzee (*Pan troglodytes*). *American Journal of Primatology*, **70**, 966-975. <http://dx.doi.org/10.1002/ajp.20589>
- [31] Wang, Y.K., Nash, M.P., Pullan, A.J., Kieser, J.A. and Röhrle, O. (2013) Model-Based Identification of Motion Sensor Placement. *Biomechanics and Modeling in Mechanobiology*, **12**, 383-399. <http://dx.doi.org/10.1007/s10237-012-0407-6>
- [32] O'Reilly, P.M.R. and Fitzgerald, M.J.T. (1990) Fiber Composition of the Hypoglossal Nerve in the Rat. *Journal of Anatomy*, **172**, 227-243.
- [33] Sokoloff, A. and Burkholder, S.A. (2013) Tongue Structure and Function. In: McLoon, L.K. and Andrade, F.H., Eds., *Craniofacial Muscles*, Chapter 12, Springer, New York, 207-227.
- [34] Langdon, H., Langdon, K. and Barnwell, Y. (1978) The Anatomy of M. Genioglossus in the 15-Week Human Fetus. *Anatomy and Embryology*, **155**, 107-113. <http://dx.doi.org/10.1007/BF00315735>
- [35] Miyawaki, K. (1973) A Study on the Musculature of the Human Tongue. *Annual Bulletin*, **8**, 23-49.

## Abbreviations

Lo: Longitudinal muscle of the tongue  
sLo: Superior longitudinal muscle of the tongue  
iLo: Inferior longitudinal muscle of the tongue  
Tr: Transverse muscle of the tongue  
Ve: Vertical muscle of the tongue  
Sty: Styloglossus muscle of the tongue  
Hyo: Hyoglossus muscle of the tongue  
Gl: Glandular tissue  
Ge: Genioglossus muscle of the tongue  
MS: Median sulcus of the tongue  
HB: Hyoid bone  
LS: Lingual septum of the tongue  
CP: Circumvallate papilla  
IE: Intermolar eminence

## Abbreviations of Temporary Names in This Paper

mMS: Muscle fascicle just under the MS  
cCP: Unknown structure in conjunction with the CP  
cTr: Unknown structure in conjunction with the Tr  
sLoG: Group of sLo and Hyo  
iLoG: Group of iLo and Sty